Available online at www.sciencedirect.com
ScienceDirect
Journal of Fluorine Chemistry 128 (2007) 269–276
JOURNAL OF FLUORINE CHEMISTRY
www.elsevier.com/locate/fluor

Electrodeposition of fluorine-doped lead dioxide

A.B. Velichenko [a,*], D. Devilliers [b]

[a] Department of Physical Chemistry, Ukrainian State Chemical Technology University, Gagarin ave. 8, Dnepropetrovsk 49005, Ukraine
[b] Université Pierre et Marie Curie-Paris 6, Laboratoire LI2C-Electrolytes et Electrochimie 4, Place Jussieu-75252 Paris Cedex 05, France

Received 11 August 2006; received in revised form 14 November 2006; accepted 22 November 2006
Available online 25 November 2006

Abstract

The electrocatalytic properties of PbO_2 may be increased by incorporation of some ions such as F^-. In this review, the preparation of fluorine-doped PbO_2 in the presence of some additives of fluorine-containing compounds (F^-, potassium salt of nonafluoro-1-butanesulfonic acid $C_4F_9O_3SK$ and Nafion®) is reported. The mechanism of electrodeposition is discussed. The amount of additives in the deposit depends on the experimental conditions: potential, current density and charge of additive species in the plating solution. The physicochemical properties of doped oxide are very different from those of undoped oxide, accounting for the different electrocatalytic activity of the materials.

Keywords: Fluorine-doped; Composite; Lead dioxide; Electrodeposition

1. Introduction

There is a great interest in the improvement of lead dioxide as an electrode material for use in different applications, for instance, in lead–acid battery, an analytical transducer with a high electrocatalytic activity for anodic oxygen transfer processes, ozone evolution, electrosynthesis and waste treatment processes. Electrodeposited pure lead dioxide was demonstrated to exhibit a moderate electrocatalytic activity toward various anodic reactions in acidic media. However, this activity can often be enhanced greatly by incorporation of some ions, for example Bi^{3+}, As^{3+}, Fe^{3+}, Cl^-, F^- [1–6]. There is not much information on effects of polyelectrolyte and surfactant additives on the process of oxide electrodeposition and the physicochemical properties of the resulting materials [4–6]. It was shown [7–9] that both polyelectrolytes and anionic surfactants are adsorbed on PbO_2 formed composite materials oxide–polyelectrolyte and oxide–surfactant with new physicochemical properties. Unfortunately, in most cases, details on the nature of the effect of these additives on the doped and composite oxide formation are not known, although there is a vast literature on the mechanism of pure lead dioxide electrodeposition [10–16].

In the present review, we report the electrodeposition of lead dioxide in the presence of some additives of fluorine-containing compounds: F^-, potassium salt of nonafluoro-1-butanesulfonic acid $C_4F_9O_3SK$ (anionic surfactant) and Nafion® (anionic polyelectrolyte).

2. Electrodeposition

According to [17,18], the presence of different ionic additives in the electrodeposition solution causes only a slight shift in the electrodeposition rate of lead dioxide without seemingly changing the deposition mechanism, which was described by the following scheme:

$$H_2O \rightarrow OH^{\bullet} + H^+ + e^- \quad (1)$$

$$Pb^{2+} + OH^{\bullet} \rightarrow Pb(OH)^{2+} \quad (2)$$

$$Pb(OH)^{2+} + H_2O \rightarrow Pb(OH)_2{}^{2+} + H^+ + e^- \quad (3)$$

$$Pb(OH)_2{}^{2+} \rightarrow PbO_2 + 2H^+ \quad (4)$$

The first stage is the formation of oxygen-containing particles as OH_{ads}, chemisorbed on the electrode. In a subsequent chemical stage, these particles interact with lead species forming a soluble intermediate product, $Pb(OH)^{2+}$ which is further oxidized electrochemically with transfer of the second electron forming a soluble oxidized Pb(IV) compound. The latter is

* Corresponding author. Tel.: +380 562 477974; fax: +380 562 477974.
E-mail address: velichenko@ukr.net (A.B. Velichenko).

0022-1139/$ – see front matter
doi:10.1016/j.jfluchem.2006.11.010

decomposed chemically to form colloidal PbO_2 particles in the electrolyte volume that crystallize on the surface. At low overpotential, the rate-determining stage is the second electron transfer reaction and at high overpotential, the process is controlled by diffusion of Pb^{2+}. To further support the reaction mechanism, effective activation energy of the reaction was calculated and impedance measurements were performed [19]. It was shown that the effective activation energy of the reaction was 70 kJ/mol at low overpotential, and it decreased with increasing electrode potential up to 13 kJ/mol.

Typical voltamograms for Pt electrode in the presence of Pb^{2+}, with and without added F^- ions, are shown in Fig. 1. The anodic branch of the curve, at potentials more positive than 1.45 V, features an important current growth that corresponds to the simultaneous reactions of Pb(II) oxidation and oxygen evolution [14–19]. In the cathodic branch of the curve, in the range 1.0–1.2 V, one can observe a current peak due to reduction of lead dioxide. From gravimetric measurements, we established that the area and the magnitude (I_p) of the reduction peak are a good measure of the amount of lead dioxide deposited on the electrode surface [14–19]. In the presence of F^- the cathodic peak of lead dioxide dissolution increases (Fig. 1) indicating, according to [14–19], an increase in the PbO_2 deposition rate. We observed the similar effect when Nafion® was added in the deposition solution instead of F^-. At the same time potassium salt of nonafluoro-1-butanesulfonic acid hardly influenced the *i–E* curve [20].

Typical partial steady-state polarization curves (PbO_2 electrodeposition only) for Pt in the presence of Pb^{2+} in the HNO_3 solution are shown in Fig. 2. The current efficiency of the lead dioxide (CE_{PbO_2}) and the PbO_2 electrodeposition current (I_{PbO_2}) were calculated from equations [14–19]:

$$CE_{PbO_2} = \frac{Q_{red}}{Q} \tag{5}$$

$$I_{PbO_2} = \frac{Q_{red}}{t} \tag{6}$$

where Q is the total charge passed during the anodic polarization, Q_{red} is the charge passed on PbO_2 reduction at $E = 0.8$ V, t is the total time of an anodic polarization.

In the potential range 1.3–1.6 V, the current increases according to an exponential law. In this region, the current efficiencies of PbO_2 formation are in range 90–98% and in most cases we practically did not observe differences in the current values between the total and the partial curves [7,8,20–22]. This indicates that in the mentioned potential interval lead dioxide formation is the unique electrochemical process. The Tafel plot of E versus $\log(i)$, obtained from partial steady-state polarization curve (corrected from the contribution of oxygen evolution) has a slope of about 120 mV/dec [7,8,20–22]. These results are in good agreement with the data [14–19] where it was shown that at low overpotential the PbO_2 electrodeposition is limited by the second electron transfer stage (3).

The nature of additives in the solution has an effect on the partial current value in the *i–E* steady-state curves. Thus, the PbO_2 electrodeposition current increases in the presence of F^- or Nafion® (Fig. 2) in the solution and it slightly decreases when potassium salt of nonafluoro-1-butanesulfonic acid was added [5–7,20–22]. A quantitative description of lead dioxide electrodeposition in the presence of the additives is provided by the rate constant (k) of the slow kinetic stage (the second electron transfer stage), obtained from extrapolation of the linear plot of $1/I$ versus $1/\omega^{1/2}$:

$$\frac{1}{I} = \frac{1}{nkFSc_b} + \frac{1}{0.62nFSD^{\frac{2}{3}}v^{-\frac{1}{6}}c_b} \times \frac{1}{\omega^{\frac{1}{2}}} \tag{7}$$

where, v is the kinematic viscosity of the electrolyte solution ($cm^2\ s^{-1}$), ω is the angular velocity of electrode rotation (rad s^{-1}), S is the electrode area, n is the effective number of electrons exchanged in the reaction, all other terms have their usual electrochemical significance.

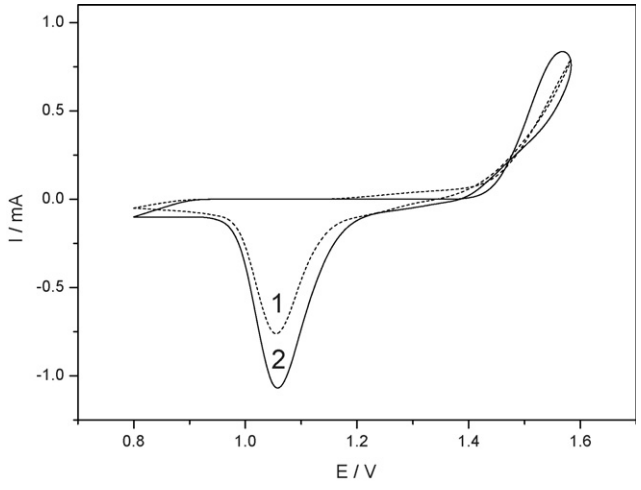

Fig. 1. Cyclic voltammograms of Pt electrode in solutions: (1) 0.1 M HNO_3 + 0.01 M $Pb(NO_3)_2$; (2) 0.1 M HNO_3 + 0.01 M $Pb(NO_3)_2$ + 0.01 M NaF. $v = 100$ mV s^{-1}. $S = 0.2$ cm^2.

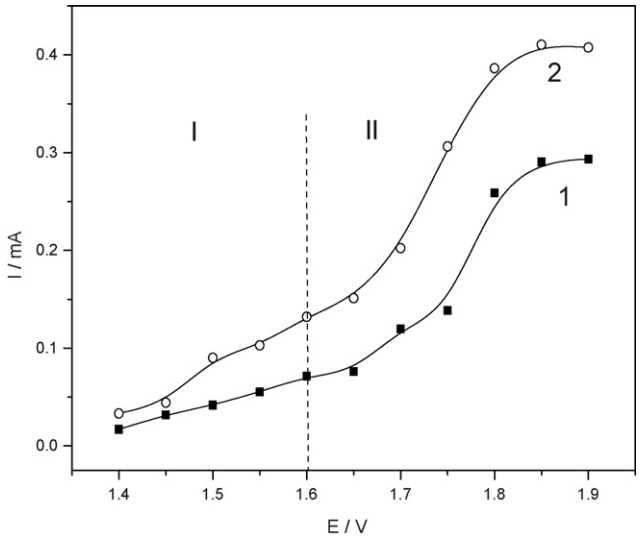

Fig. 2. Steady-state polarization curves of Pt electrode for partial current of PbO_2 electrodeposition in solutions: (1) 0.1 M HNO_3 + 0.01 M $Pb(NO_3)_2$; (2) 0.1 M HNO_3 + 0.01 M $Pb(NO_3)_2$ + 0.0001 wt.% Nafion®. $S = 0.2$ cm^2.

Table 1
Rate constants for Pb(II) oxidation (E = 1.800 V)

Electrodeposition solution	β	$k \times 10^4$ (m s^{-1})
0.1 M HNO_3 + 0.01 M Pb^{2+}	0.4	4.1
0.1 M HNO_3 + 0.01 M Pb^{2+} + 0.01 M F^-	0.4	5.7
0.1 M HNO_3 + 0.01 M Pb^{2+} + 0.003 M $C_4F_9O_3SK$	0.4	3.5
0.1 M HNO_3 + 0.01 M Pb^{2+} + 0.0001 wt.% Nafion®	0.4	11.2

Experimental and calculated kinetic parameters (β, k) in the absence and in the presence of additives [5–7,20–22] are summarised in Table 1. We point out that the values of the constants in Table 1 are qualitatively in good agreement with voltammetric data (Figs. 1 and 2). Increase of the additive content in the deposition solution leads to decrease of the constant rate for $C_4F_9O_3SK$ and to increase for F^-. More complex relationship between the constant rate and the additive content is observed in case of Nafion® (Fig. 3) [7,21].

The important conclusion is that the presence of additives in the electrodeposition solution causes only a quantitative difference in the PbO_2 electrodeposition process without apparently changing the qualitative relationships, in accord with published data [17,18]. Thus, one can reasonably infer that the electrodeposition mechanism of lead dioxide from solutions containing fluorine additives is the same and can be described by reaction schemes (1)–(4).

Nafion®, $C_4F_9O_3SK$ and F^- adsorb on the positively charged PbO_2 particles [5–7,20–22]. So all observed effects have a surface nature. At low overpotentials, the influence of adsorption on the electron-transfer stage can be described by following equation [23–25]:

$$\frac{i_\theta}{i_{\theta=0}} = (1-\theta)\exp(-A\theta)\exp\left[-\frac{(z+\beta n)F\Delta\psi'(\theta)}{RT}\right] \quad (8)$$

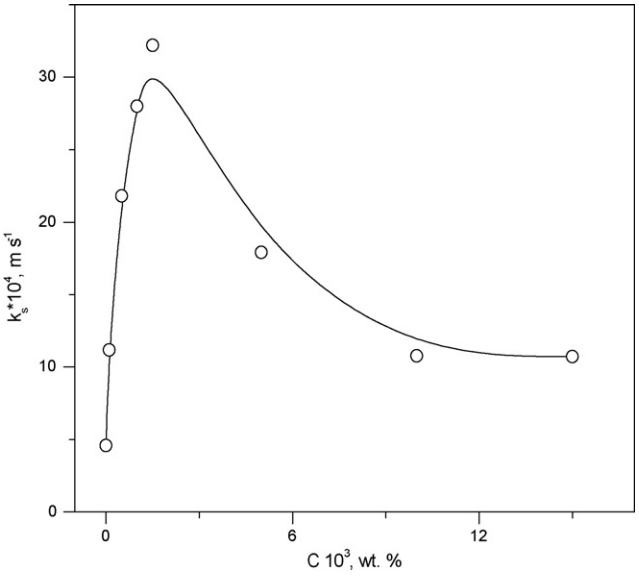

Fig. 3. Effect of the content of Nafion® additive in the electrolyte (0.1 M HNO_3 + 0.01 M $Pb(NO_3)_2$) on the constant rate of the second electron transfer stage (3).

where θ – electrode coverage by additives; A – inhibition parameter; z – charging number of the electroactive particle; n – the effective number of electrons exchanged in the reaction; β-transfer coefficient; $\Delta\psi'(\theta)$ – dependence of the ψ' – potential on electrode coverage by additives.

In the most cases, surfactants, for instance $C_4F_9O_3SK$, inhibit electrodeposition of lead dioxide due to their adsorption on the PbO_2 coating that blocks some active centers on the electrode surface where further electrochemical reaction takes place [20]. Some small ions, for example F^-, can accelerate the electrochemical process due to a lower ψ' value [5,6]. In very rare cases, we can observe both effects together [7,8,21,22]. For instance, the dependence of the constant rate for electrodeposition of PbO_2 on the concentration of Nafion® in the deposition solution has a volcano shape (Fig. 3). At low content of Nafion® in the solution, the rate constant of the process increases with increasing the additive concentration, probably due to ψ' effect. At higher Nafion® contents in the solution, the process is inhibited due to the site blocking effect.

The shape of the polarization curve, at potentials higher than 1.6 V, features an exponential current growth that corresponds to the simultaneous reactions of Pb^{2+} oxidation and oxygen evolution [14–19]. In this potential region, oxygen evolution contributes significantly to the total current thus, decreasing the current efficiency of lead dioxide formation (Fig. 4). At the same time, we observed that the increase of the electrode potential has hardly an influence on the partial current; limiting-current conditions are reached at potentials higher than 1.8 V. The value of partial current in this region strongly depends on the rotation speed of the electrode; the dependence of the current on the square root of electrode rotation speed is linear, indicating that, in this potential region, lead dioxide deposition occurs under diffusion control. The value of limiting-current strongly depends on the additive nature. In cases of F^- [5,6] and Nafion® [7,8,21,22], limiting-current increases (Fig. 2) with additive content due to migration effect [7,8]. At the same time,

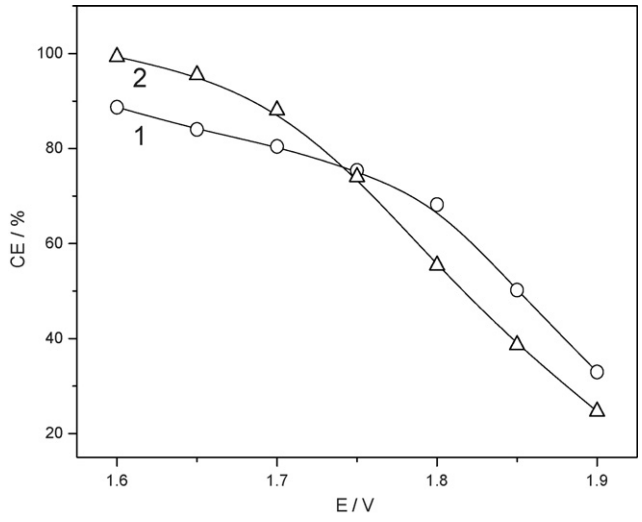

Fig. 4. PbO_2 current efficiency at Pt electrode in solutions: (1) 0.1 M HNO_3 + 0.01 M $Pb(NO_3)_2$; (2) 0.1 M HNO_3 + 0.01 M $Pb(NO_3)_2$ + 0.0001 wt.% Nafion®. S = 0.2 cm^2.

$C_4F_9O_3SK$ addition leads to decrease of limiting-current as the result of the decrease of effective electrode surface (blocking effect) [20].

3. Chemical composition

Additive incorporation into the PbO_2 deposits does occur, and their content strongly depends on the concentration in the electrolyte and on the electrodeposition conditions [5–8,17,18,20–22]. In most cases, additive content in the oxide increases proportionally to the concentration in the electrodeposition solution. It is important to note that electrode potential or current density is strongly influenced by the additive content in the electrodeposited material. Taking into account the values of additives involved, we can advance the plausible explanation that the process of ion incorporation into lead dioxide involves the physical adsorption of ionic species and surfactants or the chemical adsorption of polyelectrolytes on the growing oxide deposit [5–8,17,18,20–22].

It is interesting to note that all kinds of additives (ionic-F^-, surfactant-$C_4F_9O_3SK$ and polyelectrolyte-Nafion®) are incorporated into the deposited lead dioxide forming doped or composite oxide [5–8,20–22]. The additive content in the lead dioxide can change from 1 wt.% to 20 wt.% depending on the electrodeposition conditions and the electrolyte composition (Fig. 5; Tables 2 and 3). The additive contents in the oxide increase proportionally to the concentration in the deposition solution (Table 3, Fig. 5).

As already anticipated by the data in Fig. 5, the deposition current density represents an important factor in determining the additive amount that is incorporated into the electrochemically grown PbO_2. Based on these data and evidence reported below, and taking into account the dependence on additive content in the solution, we can advance the plausible

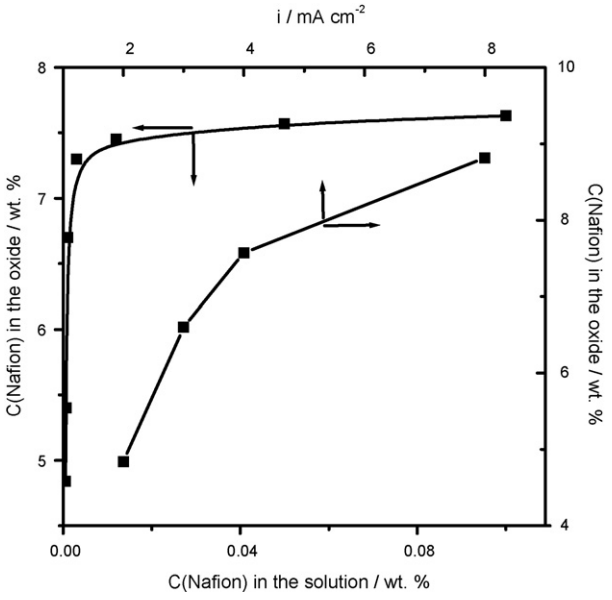

Fig. 5. Effect of deposition current density (i) and concentration of polymeric additive (C_{Nafion}) on the Nafion® content in the composite material.

Table 2
Fluoride-ion content in PbO_2

Electrodeposition solution	F^- content (at.%)
0.1 M HNO_3 + 0.01 M Pb^{2+} + 0.01 M F^-	1.0
0.1 M HNO_3 + 0.01 M Pb^{2+} + 0.02 M F^-	3.0
0.1 M HNO_3 + 0.01 M Pb^{2+} + 0.03 M F^-	4.5

explanation that the process of additive incorporation into lead dioxide involves the physical adsorption of ionic species (negatively charged) on the growing oxide deposit. Since the reported value of the zero charge potential for PbO_2 in nitrate solutions is 0.91 ± 0.1 V versus SCE [26], in our deposition conditions, the electrode surface is always positively charged. On increasing the current density, the additive content strongly increases (Fig. 5) due to the fact that the electrode charge becomes more positive. We can observe the same effect at high acid concentration in the deposition solution (Table 3).

It is important to note that addition of fluoride ions, together with Fe^{3+} or Co^{2+} in the electrodeposition solution leads to an increase of the amount of fluoride incorporated into PbO_2 [17,18]. At the same time, the dependence of the Fe or Co content in PbO_2 on the current density and pH of electrolyte is rather similar to the system that is doped only with iron or cobalt, where an increase of the current density and/or pH of electrolyte leads to a decrease of the Fe or Co content in the PbO_2 bulk. This indicates the F-containing complex still has positive charge: it is likely a complex fluoride with iron such as $[Fe(OH)_xF_y]^{(3-x-y)+}$.

Taking into account formation of colloidal PbO_2 particles during electrodeposition process, adsorption of negatively charged additives on PbO_2 particles, influence of electrolysis conditions and electrolyte composition mentioned above, we can suggest the colloidal–electrochemical mechanism of the doped and composite material formation [7,8,20–22]. It includes several electrochemical and chemical stages: electrochemical formation of oxide particles in the solutions (Eq. (9)) following reaction scheme (1)–(4); adsorption of inorganic anion, polyelectrolyte or surfactant on the oxide particles (Eq. (10)), their electrophoresis to the electrode (for particles with negative ζ-potential) with further crystallization on the anode surface

Table 3
Effect of nitric acid concentration on the additive content in the composite material ($i = 4$ mA cm^{-2})

Electrodeposition solution	Additive content (wt.%)
0.1 M HNO_3 + 0.1 M $Pb(NO_3)_2$ + 0.05 wt.% Nafion®	7.0
0.5 M HNO_3 + 0.1 M $Pb(NO_3)_2$ + 0.05 wt.% Nafion®	8.7
1.0 M HNO_3 + 0.1 M $Pb(NO_3)_2$ + 0.05 wt.% Nafion®	10.2
2.0 M HNO_3 + 0.1 M $Pb(NO_3)_2$ + 0.05 wt.% Nafion®	13.1
3.0 M HNO_3 + 0.1 M $Pb(NO_3)_2$ + 0.05 wt.% Nafion®	17.0
0.2 M HNO_3 + 0.1 M $Pb(NO_3)_2$ + 0.005 $C_4F_9O_3SK$	9.6
0.5 M HNO_3 + 0.1 M $Pb(NO_3)_2$ + 0.005 $C_4F_9O_3SK$	12.2
1.0 M HNO_3 + 0.1 M $Pb(NO_3)_2$ + 0.005 $C_4F_9O_3SK$	16.2

(Eq. (11)):

$$Pb^{2+} + 2H_2O \rightarrow PbO_{2(vol.)} + 4H^+ + 2e \quad (9)$$

$$PbO_{2(vol.)} + R \leftrightarrow PbO_2{-}R_{ads.(vol.)} \quad (10)$$

$$PbO_2{-}R_{ads.(vol.)} \rightarrow PbO_2{-}R_{ads.(sur.)} \quad (11)$$

4. Physicochemical properties

It has been previously reported [27] that variations of the conditions of PbO_2 electroplating cause changes in the oxide properties, such as the crystallographic nature, which result in a different electrocatalytic behaviour. In acidic solutions, electrodeposition of lead dioxide leads predominantly to the tetragonal β-form, although a small amount of the orthorhombic α-form is also present depending on the experimental conditions [28]. In this respect, it is important to note that the literature data on the influence of electrodeposition conditions on the crystallographic nature of the electrodeposited PbO_2 are rather contradictory. Thus, for example, the formation of α-PbO_2 was reported to be favored by relatively high deposition current densities [29], while pure β-PbO_2 was deposited at low current densities [30]. According to recent data [31] in case of acidic solutions, the PbO_2 deposits were mainly a mixture of α- and β-phases, where quantity of α-phase was on impurity level (no higher than 16%). Dependence of α-phase content on electrodeposition potential is strongly affected by the mechanism of lead dioxide electrodeposition. It increases with increasing potential in the kinetic control region and decreases in the diffusion control region. Decreasing potential and increasing temperature lead to increase in the crystallinity of the deposit and the size of grains with more preferable orientations of α- and β-grains.

To avoid any possible influence of the film thickness on the phase composition of the PbO_2 deposits [32], XRD measurements (using the Cu Kα radiation) were performed on the samples with a fixed quantity of PbO_2 (about 35 mg/cm^2). We did not observe any effects of an angle change of the X-ray beam on X-ray diffraction, indicating, as for the data of the preceding section, a uniform distribution of different forms through out the PbO_2 film thickness.

The PbO_2 film consisted of mixture of α- and β-phases of PbO_2 (Fig. 6, 1). In the case of F-doped and composite (with surfactant or polyelectrolyte) oxides, we detected mainly the β-phase of PbO_2 with different preferred orientation (Fig. 6, 2). An examination of the XRD diffractograms shows that peak intensities generally decrease with increasing additive content in the composite (see Figs. 7 and 8). This indicates that crystallinity of the composite materials is decreased due to incorporation of organic compounds. Difference in intensity provides sufficient evidence of the existence of low crystalline phase and it is in good agreement with SEM data. The SEM micrographs of F-doped PbO_2 reported in Fig. 9 show that its morphology is more regular, with better-oriented crystals of smaller size. It is important to note that in the presence of polyelectrolytes and surfactants, submicro- and nano-crystalline

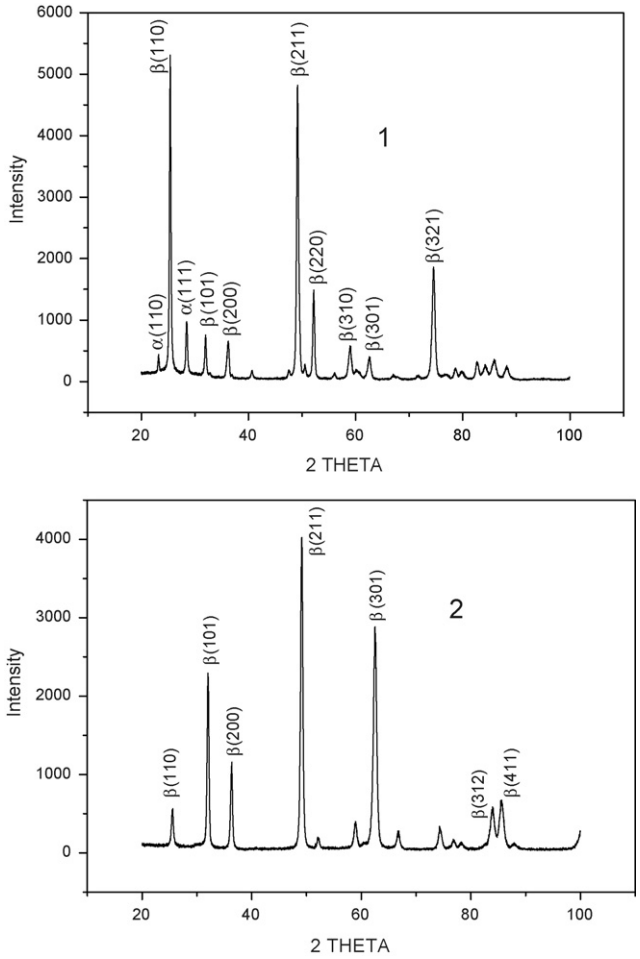

Fig. 6. X-ray diffractograms of PbO_2 films with different composition: (1) PbO_2; (2) 99% PbO_2 + 1% F^-.

coatings are formed (Fig. 9). One can suggest that the formed composite materials are mixture of two phases: crystalline PbO_2 and amorphous organic additives [7–9,20–22].

It is important to note that the oxygen-containing species and water adsorbed on the surface of an oxide electrode play very important role in electrocatalysis at high anodic potentials [33,34]: changes in the surface coverage by oxygen species, and their bond strength, cause changes in the electrocatalytic activity of the oxide electrode. It is widely held, for example, that these phenomena have a fundamental role in the reaction of ozone electrogeneration at PbO_2 electrodes [35,36]. In this respect, X-ray photoelectron spectroscopy (XPS) is a valuable technique for distinguishing different forms of oxygen-containing species adsorbed on the PbO_2 surface [37–39].

The XPS signal in the (O1s) binding energy region consists typically of a sharp peak at 527.7–528.6 eV and of a more or less pronounced shoulder at higher binding energy [38–40]. The first signal is assigned to strongly bound (lattice) oxygen; the shoulder, disappearing already after few seconds of sputtering, is assigned to more weakly bound oxygen species: adsorbed OH^- and water. In the XPS spectra of electrodeposited PbO_2, these differences are usually evident enough

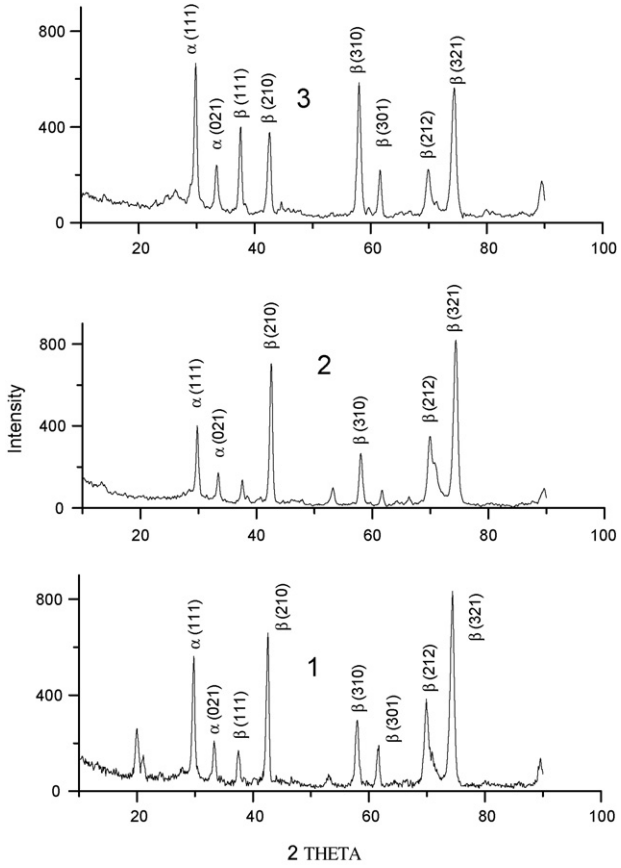

Fig. 7. X-ray diffractograms of PbO_2 films with different composition: (1) 98% PbO_2 + 2% surfactant; (2) 94% PbO_2 + 6% surfactant; (3) 86% PbO_2 + 14% surfactant.

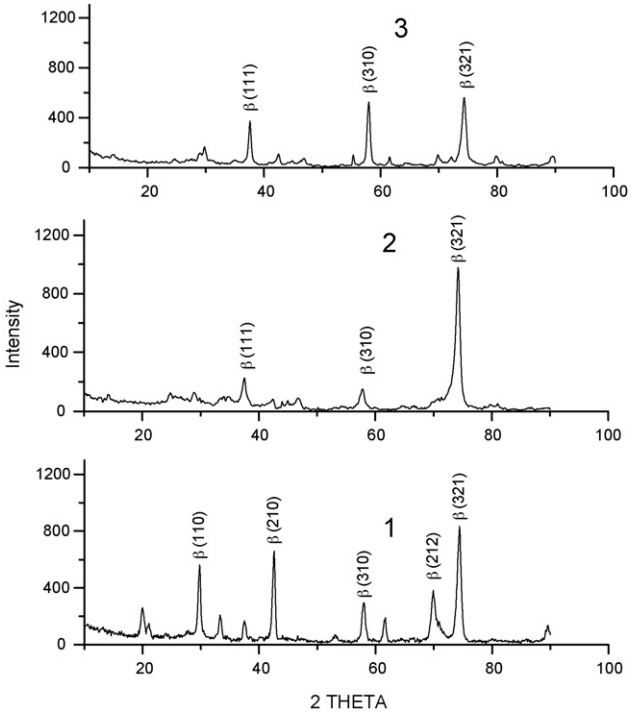

Fig. 8. X-ray diffractograms of PbO_2 films with different composition: (1) 96% PbO_2 + 4% Nafion®; (2) 93% PbO_2 + 7% Nafion®; (3) 83% PbO_2 + 17% Nafion®.

[39] as to allow us to study possible effects of doping elements on surface oxygen species in doped PbO_2 [37].

The XPS spectra in the Ols region show that doping elements cause a marked decrease of the broad signal at the higher binding energies due to adsorbed OH and H_2O [17,18]. This effect increases in the order F < Fe < (Fe^{3+} + F^-). The effect in the last case (coexistence of Fe and F) is the result of an increase of both the iron and fluoride content within PbO_2 and on the surface [37]. Conversely, neither the position of the peak at lower binding energies, assigned to oxide ions within the structure, nor that of the Pb4f undergo major changes, and the diagnostic difference, Δ(O1s–Pb4$f_{7/2}$) [37,38] is 392 ± 0.25 eV for both PbO_2 and doped PbO_2 samples. While more work is needed, the conclusion that the present data seem to bring out is that doping elements affect the weakly bound oxygen species, i.e., those ultimately involved in the O_2 evolution process [17,18].

The question that remains open concerns the understanding of the binding mode of the foreign species in PbO_2, and which sites are involved. In the case of fluoride, XPS can provide some information: a well-defined F1s peak is observed at 683.4 eV, which seems to suggest that fluoride is present in the oxide as a PbF_2-like compound [40]. It is particularly interesting, in this respect, that SIMS investigations of F-doped-PbO_2 showed the presence of clusters of the type PbOF and PbF_2 and an enrichment of fluorine in the surface region [38], in agreement with XPS data.

An association of fluorine with Pb(II) is not surprising if it is seen in the light of the models of PbO_2 proposed by Pavlov et al. [41–43] and by Giovanoli and Rüetschi [44]. The latter authors proposed the following composition formula for lead dioxide:

$$Pb^{4+}_{(1-x-y)}Pb^{2+}_{(y)}O^{2-}_{(2-4x-2y)}OH^{-}_{(4x+2y)} \quad (12)$$

where x is the cation vacancy fraction and y the fraction of Pb^{2+} ions, with respect to the total number of cationic sites. The model accounts for the fact that experimental studies report evidence for the presence of Pb(II) [45] and structural water (e.g. [46–49]) in the PbO_2 lattice. Substitution of part of the hydroxyl groups by F^-, having a similar ionic radius, was shown by radiotracer experiments [50] and by SIMS data [51], and can explain the XPS data reported in [17,18].

According to XPS data for PbO_2, which was deposited from perchloric or nitric acid solutions in the presence 0.02 M F^-, the fluoride content in the oxide bulk was about 4 at.%. For the conditions that give a uniform distribution of fluoride within the PbO_2 layer with $\Theta_{OH} + \Theta_F = 1$, the average surface coverage by fluoride was calculated to be about 6%. Using the MNDO method (Modified Neglect of Differential Overlap is a semi-empirical method for the quantum calculation of molecular electronic structure), one tried to estimate the influence of fluoride on the geometric and electronic factors of the modified PbO_2 surface, and on the metal–oxygen intermediate bond strength on the process of O_2 evolution [5,52]. As a model of the PbO_2 surface one adopted the structure indicated as Cluster I (Fig. 10). Two adjoining oxygen species take part in the oxygen

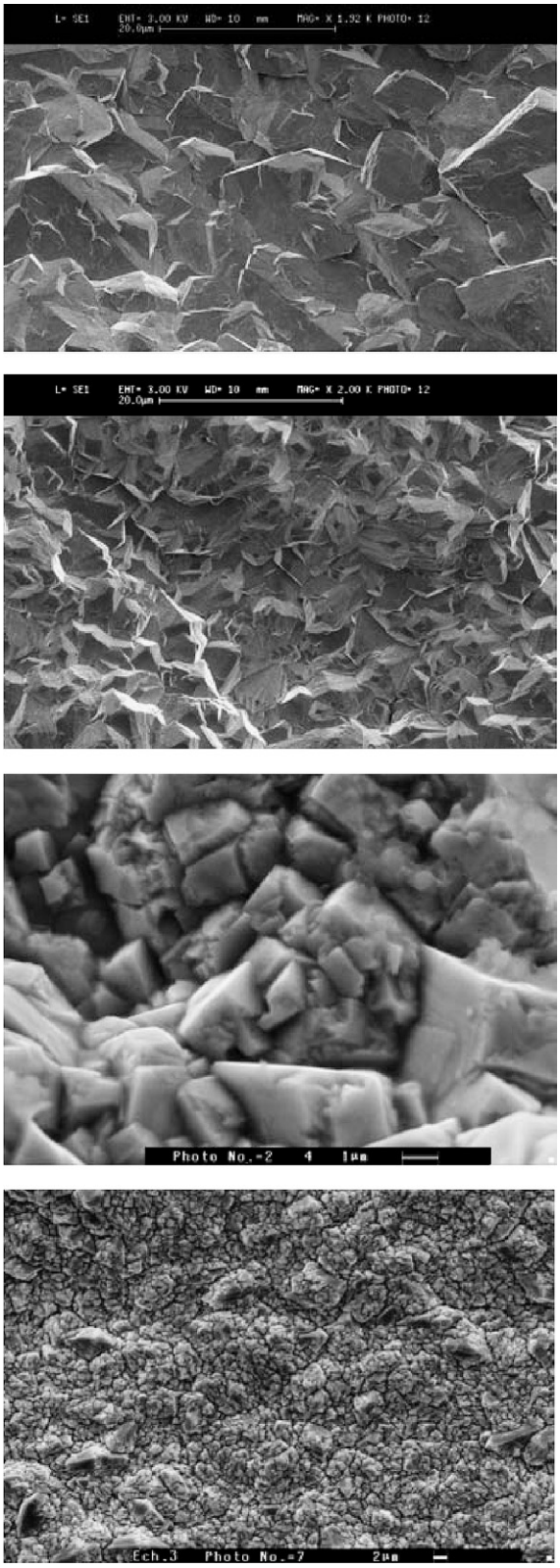

Fig. 9. SEM micrographs of PbO_2 films with different composition: (1) PbO_2; (2) 97% PbO_2 + 3% F^-; (3) 94% PbO_2 + 6% surfactant; (4) 83% PbO_2 + 17% Nafion®.

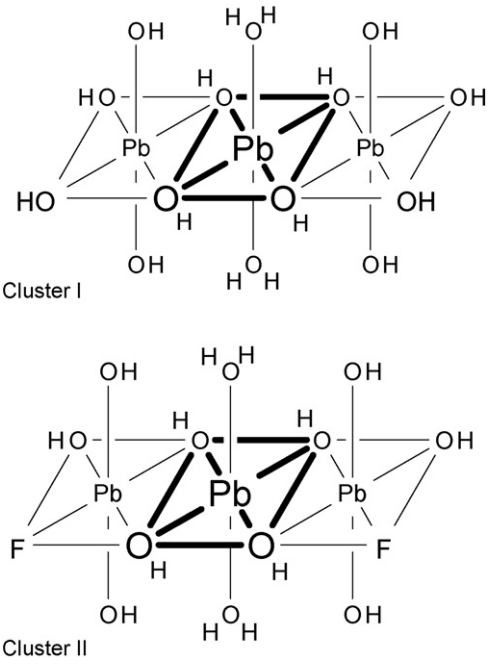

Fig. 10. Cluster models used for MNDO calculations on the effects of oxygen substitution with fluorine.

evolution process (Fig. 10, boldface lines in the Cluster I). In the simulation of fluoride modified PbO_2, two OH^- ions are replaced by two fluoride ions (Fig. 10, Cluster II). In this case, we expect the maximum influence of fluoride on the system parameters. Actually, the calculation showed that influence of fluoride on properties of electronic system is essentially negligible [5,52].

Calculations for Cluster I and Π demonstrated that fluoride shows no influence on the energy parameters for evolution of O_2 from H_2O [5,52]. Thus, within the limitations of the model, the relatively high surface concentration of fluoride versus its negligible influence on the electronic and the energy properties of the studied system, seems to suggest that the effect of the modification by fluoride is mainly that of changing the surface coverage of adsorbed oxygen species.

By comparison with unmodified PbO_2, F-doping shifts the O_2 evolution process to higher potentials for a given current; for the higher F-doping levels; however, this increase is seen mainly at the smaller currents. On the other hand, as the concentration of F in the PbO_2 growth solution is increased, the current efficiency of O_3 formation first rises and then declines to lower values.

5. Conclusions

In all cases the electrodeposition process obeys the basic relationship mentioned previously for Pt electrodes in $HClO_4$ and HNO_3 solutions, and is described satisfactorily by the kinetic scheme given in (1)–(4). The important conclusion is that the presence of additives in the electrodeposition solution causes only a quantitative difference in the PbO_2 electrodeposition process without apparently changing the qualitative relationships.

The amount of additives incorporated in the bulk of PbO_2 strongly depends on two important factors: (i) the charge of the electrode surface, hence the electrodeposition potential or

current density, and the specific adsorption of different compounds; (ii) the charge of additive species in the solution. The increase of the electrode surface charge leads to an increase of the additive content in PbO_2 bulk. The results can be tentatively explained by the adsorption of the foreign species onto the PbO_2.

The surface analysis data (XRD, SEM) indicates big differences in physicochemical properties of doped and composite PbO_2 in comparison with undoped oxide, which can account for the changes in the electrocatalytic activity observed in the range of high positive potentials.

Acknowledgement

A.B.V. thanks the Université Pierre et Marie Curie for the financial support.

References

[1] N.V. Korovin, E.V. Kasatkin, Electrokhimiya 29 (1993) 448–460.
[2] I.H. Yeo, Y.S. Lee, D.C. Johnson, Electrochim. Acta 37 (1992) 1811–1815.
[3] H. Chang, D.C. Johnson, J. Electrochem. Soc. 137 (1990) 507–510.
[4] A.B. Velichenko, D.V. Girenko, R. Amadelli, F.I. Danilov, Russ. J. Electrochem. 34 (1998) 325–328.
[5] R. Amadelli, L. Armelao, A.B. Velichenko, N.V. Nikolenko, D.V. Girenko, S.V. Kovalyov, F.I. Danilov, Electrochim. Acta 45 (1999) 757–765.
[6] A.B. Velichenko, D.V. Girenko, S.V. Kovalyov, A.N. Gnatenko, R. Amadelli, F.I. Danilov, J. Electroanal. Chem. 454 (1998) 205–210.
[7] A.B. Velichenko, T.V. Luk'yanenko, R. Amadelli, F.I. Danilov, Ukr. Chem. J. 70 (3) (2004) 51–56.
[8] A.B. Velichenko, T.V. Luk'yanenko, F.I. Danilov, R. Amadelli, D. Devilliers, Proceeding of 6th International Conference on Lead-Acid Battery (LABAT'2005), Varna, Bulgaria. 13–16 June, 2005.
[9] A.B. Velichenko, T.V. Luk'yanenko, R. Amadelli, D. Devilliers, F.I. Danilov, Proceeding of 3rd Gerischer-Symposium on Electrocatalysis, Berlin, Germany. 6–8 July, 2005.
[10] M. Fleischmann, J.R. Mansfield, H.R. Thirsk, H.G.E. Wilson, Electrochim. Acta 12 (1967) 967–982.
[11] H. Chang, D.C. Johnson, J. Electrochem. Soc. 136 (1989) 23–27.
[12] H. Chang, D.C. Johnson, J. Electrochem. Soc. 136 (1989) 17–22.
[13] S.A. Campbell, L.M. Peter, J. Electroanal. Chem. 36 (1991) 185–194.
[14] A.B. Velichenko, D.V. Girenko, F.I. Danilov, Electrochim. Acta 40 (1995) 2803–2807.
[15] A.B. Velichenko, D.V. Girenko, F.I. Danilov, J. Electroanal. Chem. 405 (1996) 127–132.
[16] A.B. Velichenko, D.V. Girenko, F.I. Danilov, Russ. J. Electrochem. 33 (1997) 96–99.
[17] A.B. Velichenko, R. Amadelli, G.L. Zucchini, D.V. Girenko, F.I. Danilov, Electrochim. Acta 45 (2000) 4341–4350.
[18] A.B. Velichenko, R. Amadelli, E.A. Baranova, D.V. Girenko, F.I. Danilov, J. Electroanal. Chem. 527 (2002) 56–64.
[19] A.B. Velichenko, E.A. Baranova, D.V. Girenko, R. Amadelli, F.I. Danilov, Russ. J. Electrochem. 39 (2003) 615–621.
[20] A.B. Velichenko, T.V. Luk'yanenko, O.V. Kravtsov, R. Amadelli, F.I. Danilov, Questions Chem. Chem. Technol. (2) (2004) 151–155 [in Russian].
[21] A.B. Velichenko, T.V. Luk'yanenko, O.V. Kravtsov, R. Amadelli, F.I. Danilov, Questions Chem. Chem. Technol. (2) (2003) 114–118 [in Russian].
[22] A.B. Velichenko, T.V. Luk'yanenko, R. Amadelli, G.V. Korshin, O.V. Kravtsov, F.I. Danilov, Questions Chem. Chem. Technol. (4) (2003) 106–111 [in Russian].
[23] A.N. Frumkin, Doklady AN SSSR 85 (1952) 373–376.
[24] B.B. Damaskin, Electrode Processes in Solutions of Organic Compounds, MSU, Moscow, 1985.
[25] M.A. Loshkaryov, F.I. Danilov, G.E. Bol, L.G. Sechin, Electrokhimiya 13 (1977) 593–596.
[26] A.J. Bard, Encyclopedia of Electrochemistry of the Elements, vol. II., Marcel Dekker Inc., New York, 1973, pp. 235–346.
[27] J.C.G. Thanos, D.W. Wabner, J. Electroanal. Chem. 182 (1985) 25–36.
[28] N. Munichandraiah, J. Appl. Electrochem. 22 (1992) 825–829.
[29] R. Stevens, D. Gilroy, J. Microscopy 124 (1981) 265–274.
[30] J.P. Carr, N.A. Hampson, R. Taylor, J. Electroanal. Chem. 27 (1970) 109–113.
[31] A.B. Velichenko, R. Amadelli, A. Benedetti, D.V. Girenko, S.V. Kovalyov, F.I. Danilov, J. Electrochem. Soc. 149 (2002) C445–C449.
[32] I. Petersson, E. Ahlberg, B. Berghult, J. Power Sources 76 (1998) 98–105.
[33] S. Trasatti, Electrochim. Acta 29 (1984) 1503–1512.
[34] S. Trasatti, G. Lodi, Electrodes of Conductive Metallic Oxides. Part B., Elsevier, Amsterdam, 1981, pp. 521–626.
[35] P.C. Foller, C.W. Tobias, J. Phys. Chem. 85 (1981) 3238–3244.
[36] P.C. Foller, C.W. Tobias, J. Electrochem. Soc. 129 (1982) 506–515.
[37] R. Amadelli, L. Armelao, E. Tondello, S. Daolio, M. Fabrizio, C. Pagura, A. Velichenko, Appl. Surf. Sci. 142 (1999) 200–203.
[38] K.S. Kim, T.J. O'Leary, N. Winograd, Anal. Chem. 45 (1973) 2214–2218.
[39] P. Veluchamy, H. Minoura, Appl. Surf. Sci. 126 (1998) 241–245.
[40] J.F. Moulder, W.F. Stickle, P.E. Sobol, K.D. Bomben, Handbook of X-ray Photoelectron Spectroscopy, 2nd Ed., Physical Electronics, Eden Prairie, 1995.
[41] D. Pavlov, I. Balkanov, T. Halachev, P. Rachev, J. Electrochem. Soc. 136 (1989) 3189–3198.
[42] D. Pavlov, I. Balkanov, J. Electrochem. Soc. 139 (1992) 1830–1836.
[43] D. Pavlov, J. Electrochem. Soc. 139 (1992) 3075–3080.
[44] R. Giovanoli, P. Rüetschi, J. Power Sources 13 (1991) 81–97.
[45] K.D. Naegele, W.J. Plieth, Electrochim. Acta 25 (1980) 241–247.
[46] S.M. Caulder, J.S. Murday, A.C. Simon, J. Electrochem. Soc. 120 (1973) 1515–1518.
[47] P.T. Moseley, J.L. Hutchison, C.J. Wright, M.A.M. Bourke, R.J. Hill, V.S. Rainey, J. Electrochem. Soc. 130 (1983) 829–834.
[48] P. Boher, P. Garnier, J.R. Gavarri, J. Solid State Chem. 52 (1984) 146–155.
[49] R.J. Hill, M.R. Houtchin, Electrochim. Acta 30 (1985) 559–561.
[50] R. Amadelli, G.L. Zucchini, A.B. Velichenko, *Conference on Electrified Interfaces*, Povoa de Varzim (Portugal), 5–10 July, 1988, abstract P3.
[51] R. Amadelli, A.B. Velichenko, E. Tondello, L. Armelao, S. Daolio, M. Fabrizio, Int. J. Mass Spectrom. 179–180 (1998) 309–317.
[52] A.B. Velichenko, D.V. Girenko, N.V. Nikolenko, R. Amadelli, E.A. Baranova, F.I. Danilov, Russ. J. Electrochem. 36 (2000) 1216–1220.